Computers, Materials & Continua CMC, vol.64, no.1, pp.651-664, 2020

Research on Efficient Seismic Data Acquisition Methods Based on Sparsity Constraint

Caifeng Cheng[1, 2], Xiang'e Sun[1, *], Deshu Lin[3] and Yiliu Tu[4]

Abstract: In actual exploration, the demand for 3D seismic data collection is increasing, and the requirements for data are becoming higher and higher. Accordingly, the collection cost and data volume also increase. Aiming at this problem, we make use of the nature of data sparse expression, based on the theory of compressed sensing, to carry out the research on the efficient collection method of seismic data. It combines the collection of seismic data and the compression in data processing in practical work, breaking through the limitation of the traditional sampling frequency, and the sparse characteristics of the seismic signal are utilized to reconstruct the missing data. We focus on the key elements of the sampling matrix in the theory of compressed sensing, and study the methods of seismic data acquisition. According to the conditions that the compressed sensing sampling matrix needs to meet, we introduce a new random acquisition scheme, which introduces the widely used Low-density Parity-check (LDPC) sampling matrix in image processing into seismic exploration acquisition. Firstly, its properties are discussed and its conditions for satisfying the sampling matrix in compressed sensing are verified. Then the LDPC sampling method and the conventional data acquisition method are used to synthesize seismic data reconstruction experiments. The reconstruction results, signal-to-noise ratio and reconstruction error are compared to verify the seismic data based on sparse constraints. The LDPC sampling method improves the current seismic data reconstruction efficiency, reduces the exploration cost and the effectiveness and feasibility of the method.

Keywords: Sparsity constraint, high efficient acquisition, compressed sensing, sampling matrix.

1 Introduction

Seismic data acquisition is the basis of the entire seismic exploration process, and the improvement of acquisition technology level is of great significance to the development of the entire seismic exploration. Current seismic data acquisition is based on the Fourier

[1] School of Electronics and Information, Yangtze University, Jingzhou, 434023, China.

[2] College of Engineering and Technology, Yangtze University, Jingzhou, 434020, China.

[3] School of Computer Science, Yangtze University, Jingzhou, 434023, China.

[4] Department of Mechanical and Manufacturing Engineering, University of Calgary, Calgary, Canada.

[*] Corresponding Author: Xiang'e Sun. Email: 201773029@yangtzeu.edu.cn.

Received: 23 January 2020; Accepted: 11 April 2020.

transform and the Nyquist sampling theorem [Marks (1991)]. However, the information acquisition, storage, fusion, processing and transmission under the guidance of this theory has become one of the main bottlenecks in the current information technology development, and its performance in seismic data acquisition is also obvious.

In actual exploration, the demand for 3D seismic data acquisition is increasing, and the requirements for data are becoming higher and higher. Accordingly, the acquisition cost and data volume also increases. Therefore, under the premise of meeting the data acquisition requirements, how to collect data economically and efficiently is a very urgent problem. In recent years, the theory of compressed sensing has received wide attention due to its unique advantages. It exploits the properties of data sparsely expressed, using sparse random sampling far below the traditional Nyquist sampling rate, and reconstructs the complete data signal through the sparse constrained optimization algorithm [Donoh (2006); Candes and Wakin (2008)]. The sparsity of the signal is the basis for sampling. The sampling interval of the signal depends on the structure and distribution of the information in the signal. On the one hand, the method breaks through the limitation of the Nyquist sampling theorem, breaks up the distribution of sampling aliases, and establishes a theoretical basis for widening the frequency of the signal; on the other hand, it uses less sampling and reduces the signal data human and material input in collection, transmission, storage, etc. It provides a theoretical basis for solving the problem of information redundancy and low sampling efficiency caused by the conventional sampling method. Since the compressed sensing utilizes the sparsity of the signal, it is also referred to, herein, as the signal sampling theory based on sparse constraints.

Based on the seismic sensing technology of compressed sensing, more applied research and experiments have been carried out at home and abroad. However, there are relatively few literatures on seismic acquisition data acquisition based on compressed sensing and on observation system design. Hennenfent et al. [Hennenfent and Herrmann (2008)] proposed an under-sampling method based on random jitter, which controls the maximum distance between adjacent measuring points. Moshe et al. [Mosher, Kaplan and Janiszewski (2012)] proposed and improved a non-uniform sampling method based on constraints in the design of the observation system to select the location of the excitation point and the receiving point. The non-uniform optimization sampling observation system was designed and carried out at sea and land. The data acquisition, through data reconstruction, achieved good results. The idea of applying compressed sensing to multi-source seismic data acquisition was proposed [Lin and Herrmann (2009)]. Moldoveanu [Moldoveanu (2010)] conducted a positive exploration of stochastic observation methods for maritime data acquisition. The Poisson disk sampling method [Tang (2010)] was introduced to control the separation distance between sampling seismic traces, which improved the shortcomings of the simple random sampling method used in current compressed sensing technology. Milton et al. [Milton, Trickett and Burroughs (2011)] proposed a data acquisition method for changing the conventional rule-intensive shots to random sparsely arranged shots; Ma et al. [Ma (2011); Su, Sheng, Xie et al. (2019)] proposed a viewpoint of sparse promotion of seismic exploration. As far as the concept of using compressed sensing to reduce the amount of data collected in the field, Cheng et al. [Cheng, Chen and Wang (2015)] reported the preliminary framework for applying the theory of compressed sensing to the efficient collection of seismic data. Mosher et al. [Mosher, Kaplan and Janiszewski (2012)] proposed a non-uniformity based on the theory of compressed sensing. The optimized sampling seismic data observation system design shows that the same number of instruments can be used to achieve higher spatial resolution or to complete larger acquisition tasks. The above research has made a useful exploration for efficient acquisition based on compressed sensing, which provides a basic idea for the efficient collection of seismic data by using the sparseness of seismic wavefields.

An acquisition method based on the theory of compressed sensing is to realize data acquisition according to the position of the detector array in the measurement matrix, and reduce the collection point. Because the theory of compressed sensing is a process of reconstructing high-dimensional data by using low-dimensional data, the process of dimensionality reduction is accomplished by using the sampling matrix as a key factor. Therefore, we can achieve efficient data collection from the compressed sensing sampling matrix method.

2 Compressed sampling theory and method

Compressed sensing, also known as compression sensing or compressed sampling, is a technique for signal reconstruction using sparse or compressible signals [Candes and Wakin (2008)]. Or it can be said that the signal is compressed while sampling, which greatly reduces the sampling rate. Compressed sensing skips the step of acquiring samples and directly obtains a representation of the compressed signal. The CS theory utilizes many natural signals with a compact representation on a particular basis. That is, these signals are “sparse” or “compressible”. Due to this characteristic, the signal encoding and decoding framework of the compressed sensing theory is quite different from the traditional compression process, which mainly includes three aspects: signal sparse representation, coding measurement and reconstruction algorithm.

For a real-valued finite-length one-dimensional discrete-time signal, it can be seen as a column vector of a space ×1 dimension, the elements are (=1, 2, …). Any signal in space can be represented by a linear combination of ×1 dimensional base vectors. To simplify the problem, assume that these bases are normative orthogonal. Using the vector as the base matrix formed by the column vector, then any signal can be expressed as Eq. (1).

$$X = \Psi\Theta \tag{1}$$

where Θ is the projection coefficient, and $\Theta = [\theta_i] = [\langle X, \Psi_i \rangle]$ is formed by the $N \times 1$ column vector. Obviously, the equivalent representation of the same signal X and Θ, and the representation of the signal X in the time domain, Θ is the representation of the signal in the domain Ψ. If the non-zero number of Θ is much smaller, it indicates that the signal is compressible. In general, a compressible signal is a signal that can be approximated well by *K* large coefficients, that is, its coefficients developed under a certain orthogonal basis exhibit exponential decay in a certain order, with very few large coefficients and many small coefficients. This method of implementing compression by transformation is called transform coding. In the data sampling system, the sampling rate is high but the signal is compressible, and the *N* point sampling signal *X* is obtained by sampling; the complete transform coefficient $\{\theta_i\}$ is calculated by $\Theta = \Psi^T X$ transformation; the positions of *K* large coefficients are determined, and then *N*-*K* are discarded. Small coefficient encodes the values and positions of *K* large coefficients to achieve the purpose of compression.

Compressed sensing theory shows that the signal can be sampled with a minimum number of observations without losing the information needed to approximate the original signal, so that the signal is reduced in size, that is, the signal is directly sampled to obtain a compressed representation of the signal. Without the intermediate stage of *N* sampling, the purpose of compression while sampling is achieved under the condition of saving sampling and transmission cost [Su, Sheng, Liu et al. (2019)]. Candes [Candes (2008)] demonstrates that as long as the signal is sparse in an orthogonal space, the signal can be sampled at a lower frequency, and the signal ($M << N$) can be reconstructed with high probability. That is, the transform coefficient of the signal *X* of length N on an orthogonal basis or frame is sparse. Then the original solution signal *X* can be reconstructed accurately or with high probability from the observation set by using the optimization solution method [Su, Chen, Sheng et al. (2020)]. Fig. 1 is a block diagram of the signal reconstruction process based on the theory of compressed sensing.

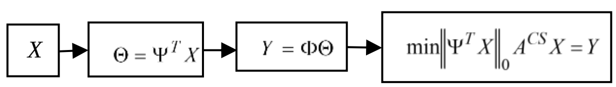

Figure 1: Signal reconstruction process of compressed sensing theory

The theory of compressed sampling states that when the signal satisfies the sparse condition or is sparse in a mathematical transformation domain, the signal can be sampled with a measurement matrix that is not related to the sparse basis, and the algorithm is used with high precision by using fewer sampling points. By continuously optimizing the reconstruction, the original signal can be recovered with high precision from fewer sampling points. The choice of sampling matrix in compressed sensing directly affects the complexity of signal sampling and reconstruction and the quality of signal recovery [Su, Sheng, Liu et al. (2020); Anandakumar and Umamaheswari (2018)].

In compressed sensing, the sampling process is non-adaptive, that is, the sampling matrix cannot change according to the change of the signal, so how to project a high-dimensional signal into a low-dimensional space without losing useful information is our research. Candes [Candes (2008)] proposed the basic standard for the sampling matrix, Restricted Isometry Property (RIP), which is defined as follows:

A is a matrix of dimension $M \times N$, if there is a constant $\delta_S \in (0,1)$, so that any signal with less than *s* non-zero elements satisfies:

$$(1-\delta_s)\|x\|_2^2 \le \|A_s x\|_2^2 \le (1+\delta_s)\|x\|_2^2 \qquad (2)$$

Then the matrix *A* is said to satisfy the *s*-order finite equidistant property with a finite equidistant constant δ_s.

In practical applications, it is easier to determine whether the sampling matrix satisfies the RIP property by correlation. The correlation refers to the maximum degree of correlation between the sampling matrix *A* and the sparse basis Ψ. The correlation $\mu(A,\psi)$ between *A* and Ψ, which can be expressed by:

$$\mu(A,\psi)=\sqrt{n}\max_{1\le i,j\le n}\left|\left\langle A_i,\psi_j\right\rangle\right| \tag{3}$$

where *n* is the column of the sampling matrix, *i* and *j* are the corresponding columns. The smaller the correlation coefficient $\mu(A,\psi)\in\left[1,\sqrt{n}\right]$, the higher the incoherence between A and ψ, and the smaller the correlation, the better the effect of the sample matrix reconstruction data. Judging by the cross-correlation parameter $\mu(\Phi)$ becomes more intuitive, which is represented by the following formula:

$$\mu(A,\psi)=\mu(\Phi)=\max_{1\le i\ne j\le n}\frac{\left|\phi_i^T\phi_j\right|}{(\left\|\phi_i\right\|_2\cdot\left\|\phi_j\right\|_2)} \tag{4}$$

where ϕ_i is the *i*-th column of Φ in the matrix. It is clear that the correlation is easier to calculate by Eq. (3) than RIP. If we normalize the columns of the matrix, we get the Gram matrix $G=\Phi^H\Phi$, and the cross-correlation parameters are transformed into the largest non-diagonal elements in G. Therefore, the cross-correlation parameter is the maximum value of the normalized inner product of the different columns in Φ.

In practical applications, for the sampling matrix we want it to have as few samples as possible, have higher sparsity, facilitate hardware implementation, and optimal recovery performance.

2.1 Seismic data regular sampling

Regular sampling (Fig. 2(a)) divides the data into different groups in equal numbers, sampling at the same position within each group, and the spacing of each sampling point is equal. If the sampling frequency is lower than the Nyquist frequency of the signal, there will be an interference frequency component phenomenon that confuses the true frequency of the signal. Therefore, one of the preconditions for compressed sampling is the random undersampling method, which converts the coherent random noise into low amplitude uncorrelated noise that is easily filtered out.

The random sampling method can overcome the aliasing caused by the conventional rule undersampling (Fig. 2(b)), which is also the inherent reason why random sampling can be used for the reconstruction of the sampled signal. Among the several sampling methods listed in Fig. 1, Gaussian random sampling tends to cause the sampling points to be too concentrated or scattered (Fig. 2(c)), causing redundancy or loss of sampling information in some areas, which brings difficulties to subsequent data recovery processing.

In order to solve the above problems, a variety of random and uniform sampling methods have been developed, and the following are commonly used:

(1) Poisson disk random sampling: Tang [Tang (2010)] control the sampling interval by setting some disks with a certain radius around adjacent sampling points (disk area cannot overlap, as shown in Fig. 2(d)).

(2) Jittered random undersampling: Firstly, all the samples are uniformly segmented, and then random “jitter” is used to select the sampling points in each segment based on the central sample points (Fig. 2(e)). This method which requires each segment to be the number of samples is odd. Compared with random sampling and regular sampling, jitter sampling takes into account the advantages of both, and ensures random sampling while

ensuring sampling spacing, avoiding the problem that adjacent sampling points are too sparse or dense [Hennenfent and Herrmann (2008)].

(3) Piecewise-random underdamping: Segment all the samples first, and then randomly select one in each sub-segment as the sampling point (Fig. 2(f)).

As a key factor of the theory of compressed sensing, the sampling matrix needs to satisfy two properties: (1) RIP property; (2) incoherence.

Candes et al. [Candes, Romberg and Tao (2006); Donoho (2006)] proposed a commonly used random sampling matrix which mainly includes the most widely used Gaussian random sampling matrix, Bernoulli sampling matrix and partial Hadamard matrix. These matrices have been proved to satisfy RIP properties, and their construction is simple. It requires less measurement to reconstruct the signal under the same conditions, but due to the uncertainty of its elements, it takes up a large memory space, which is not conducive to hardware implementation.

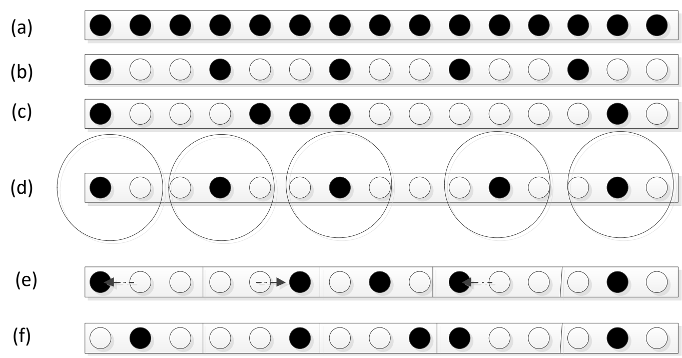

Figure 2: Schematic diagram of sampling method (5 points are sampled from 15 points) (a) All points; (b) Regular undersampling; (c) Random undersampling; (d) Poisson disk under-sampling; (e) Jittered random undersampling; (f) Piecewise-random undersampling. Solid points represent sampled points. Hollow circles represent total samples

2.2 Low-density Parity-check (LDPC) sampling matrix

2.2.1 LDPC code

It is a linear sparse code that plays a big role in the communication system and it is a code that is very close to the Shannon limit. The LDPC code has good performance in communication and image processing. It is called low density parity check code because the check matrix of the code has strong sparsity. Here we use H to represent its check Matrix. The sparsity of the code can be represented by the matrix H.

A regular LDPC code with a code length of N can be expressed as (N, λ, ρ), and λ represents the column weight in the matrix, that is, the number of non-zero elements in each column which is the number of “1”. And ρ represents the row weight of the matrix, that is, the number of non-zero elements in each row. The matrix H is usually defined by (λ, ρ), and the check matrix H must satisfy the following three conditions: (1) the row weight of each row must be ρ; (2) the column weight of each column must be λ; (3) The number of 1s in the same position in any two columns in the matrix cannot exceed “1”. The matrix satisfying these three conditions is the regular LDPC code. According to the above content, the following *H* is the LDPC rule code of the form (6, 2, 3):

$$H = \begin{bmatrix} 1 & 1 & 0 & 1 & 0 & 0 \\ 0 & 1 & 1 & 0 & 1 & 0 \\ 1 & 0 & 0 & 0 & 1 & 1 \\ 0 & 0 & 1 & 1 & 0 & 1 \end{bmatrix} \quad (5)$$

According to the above description, we can understand that the regular LDPC code can be represented by the check matrix H whose row weight is equal to each column and the column weight is equal. In some cases, the column weight and the row weight in the check matrix are not necessarily equal. The matrix in this case is called an irregular LDPC code. Through a lot of researches, the performance of the irregular code is better than the rule code, but the structure is much more complicated, so we only study the rule code here.

2.2.2 Tanner graph representation of LDPC codes

Just as the check matrix represents the LDPC code, the LDPC code can also be represented by the graph model [Yang, Zhang and Zhong (2013); Su, Sheng, Leung et al. (2019)], and the same effect as the check matrix is used to analyze the LDPC code. The rule LDPC code in the above Eq. (5) is represented by the Tanner bipartite graph as shown in the Fig. 3.

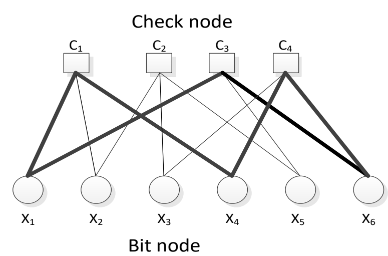

Figure 3: The Tanner bipartite graph

In the Fig. 3, C_i is called a check node and represents four row vectors of the check matrix *H*. Each row in the matrix is represented by a check node. Since there are 4 rows in the Eq. (5), there are 4 schools here. Similarly, each column in the check matrix H is represented by a variable node X_j, and the 6 variable nodes represent the 6 column vectors of the matrix *H*, so there are 6 variable nodes. When the check node is connected to the variable node, each line represents the element at the position of the *i*th row and the *j*th column of the matrix *H*, and the number of the wires represents the number of elements 1 in the matrix.

As can be seen from the Tanner graph, starting from a node in the graph, the check node and the variable node finally return to the original node, and a closed loop is formed through the connection. This loop is called the ring of the Tanner graph. The total number of wires constituting the ring is called the ring length of the Tanner graph, and the loop shown in Fig. 3 is a loop of 6 lengths (bold portion). In a Tanner graph, a total of many rings are generated. In all loops, the smallest loop length is the girth, and the performance of the LDPC code can be expressed by the girth. In the design process, in order to ensure LDPC for good performance of the code, we try to avoid loops with a loop length of 4, which will destroy the performance of the matrix, so the check matrix H needs to meet the principle of minimum loop length and the conditions of row and column (RC) constraints [Eldar, Ozols and Thompson (2020)]. In theory, when selecting the check matrix, the matrix with a longer loop length should be preferred, which also shows that each node in the matrix has higher independence. That is to say, the larger the length of the inner ring of the matrix, the higher the non-correlation between the columns in the matrix, which is also the requirement of the RIP property, indicating that the check matrix of the LDPC code conforms to the condition of the sampling matrix in the theory of compressed sensing.

2.2.3 Nature of LDPC codes

Sparsity. The LDPC code has good sparsity, and only two elements "0" and "1" are contained in the parity check matrix H of the code (N, λ, ρ). According to the above, we can see that the non-zero elements in the check matrix H are particularly small, that is, the low density of LDPC, which is what we often call sparsity.

Irrelevance. It can be seen from the bipartite graph of the LDPC code that the length of the ring in the LDPC code determines the nature of the LDPC code. When the loop length is longer, the independence between the nodes is stronger, and the incoherence of the rows and columns in the check matrix H is stronger where the incoherence also reflects the nature of RIP. In addition, the check matrix H has strong orthogonality, all of which satisfy the properties of the sampling matrix in the compressed sensing theory [Zhang and Li (2018)]. Therefore, the check matrix of the LDPC matrix can be used as a sampling matrix for compressed sampling.

3 Efficient acquisition of seismic data reconstruction experiment

In this section, we use the simulation data to perform the missing reconstruction on the above different sampling methods, and compare the results. Here we use the signal-to-noise ratio (SNR) as the criterion for judging the data recovery effect:

$$SNR = 10\log\left(\frac{\|\tilde{x}\|_2^2}{\|\tilde{x}-x\|_2^2}\right) \tag{6}$$

where $\tilde{x}$ is the original seismic data and x is the reconstructed seismic data.

We simulate seismic signals through the Ricker wavelet. The signal frequency is 15 Hz and the sampling frequency is 10 Hz, the signal length is 256. The signal is sparsely represented by Fourier transform, and reconstructed by the orthogonal matching pursuit algorithm (OMP) [Wang and Geng (2020)]. Here we compare the LDPC matrix sampling method with random sampling. The Fig. 4 shows the signal simulation at different sampling rates.

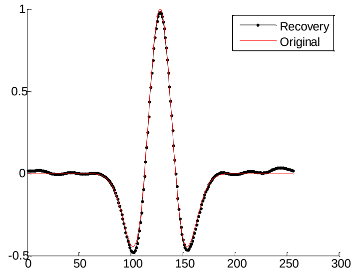

(a)

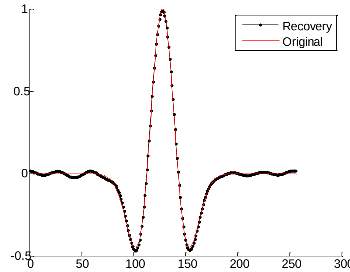

(b)

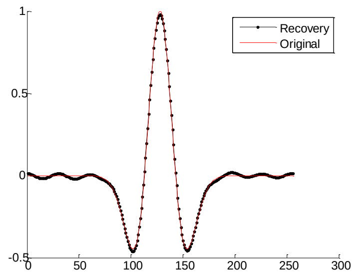

(c)

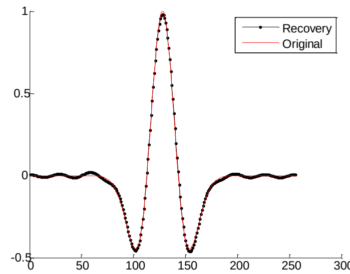

(d)

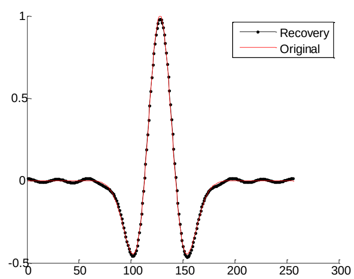

(e)

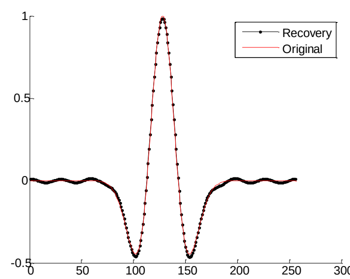

(f)

Figure 4: Ricker wavelet simulation reconstruction test under different sampling matrices (a), (c), (e) are reconstructed signals with a sampling rate of 25%, 50%, and 75% random sampling, respectively. (b), (d), (f) are reconstructed signals of sampling rate 25%, 50%, 75% LDPC sampling matrix, respectively

Table 1: SNR and Reconstruction error of three kinds of sampling simulation data under 25% of the sampling rate

Sampling method	Random sampling	Jittered sampling	LDPC sampling
Reconstruction error	0.0536	0.0487	0.0412
Reconstructed SRN	25.421	26.736	27.563

In order to reduce the error of the experiment, we performed 50 calculations for each result and averaged them. From Fig. 4 and Tab. 1, we can see that the two sampling matrices do not have much difference in signal recovery at the same sampling rate. The original signal is basically consistent with the reconstructed signal, and the two curves are basically visually viewed from the image. The data is consistent, and the data shows that the SNR difference does not exceed 0.l db. As the sampling rate increases, the SNR gradually increases, but it is not greatly affected, so even when low the sampling matrix can also reconstruct the signal well under the sampling rate. Moreover, it can be seen from the experimental results that the LDPC matrix is feasible to reconstruct the seismic data.

Subsequently, we performed the missing sampling and reconstruction of the single-shot 3D simulation data according to three different acquisition methods, and selected the same record for specific analysis. K-Singular Value Decomposition (K-SVD) was used as the sparse transformation method, and Fast Iterative Shrinkage-Thresholding Algorithm (FISTA) was used as the reconstruction algorithm [Liu, Wu, Mo et al. (2018)]. The sparse dictionary D is obtained by training the complete original record, the number of seismic traces is 90, the number of sampling points is 900, and the time sampling interval is 0.001 s. A dictionary is trained on the extracted records to obtain a corresponding representation.

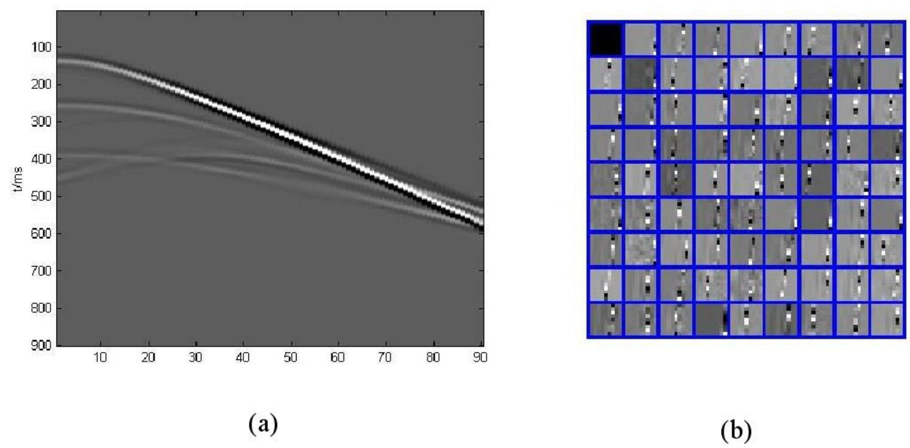

Figure 5: (a) Seismic records of one line in 3D simulation data; (b) K-SVD dictionary

According to the above three different sampling methods, we perform the missing simulation of the data. When the number of tracks is more than that of the LDPC matrix method, we can use the block method. This design is simpler than the whole region. Moreover, the randomness of the matrix design is guaranteed, and the workload required for designing a small number of lines is also reduced. In order to avoid the contingency of the results, 50 calculations are performed for each sampling method, and then averaged.

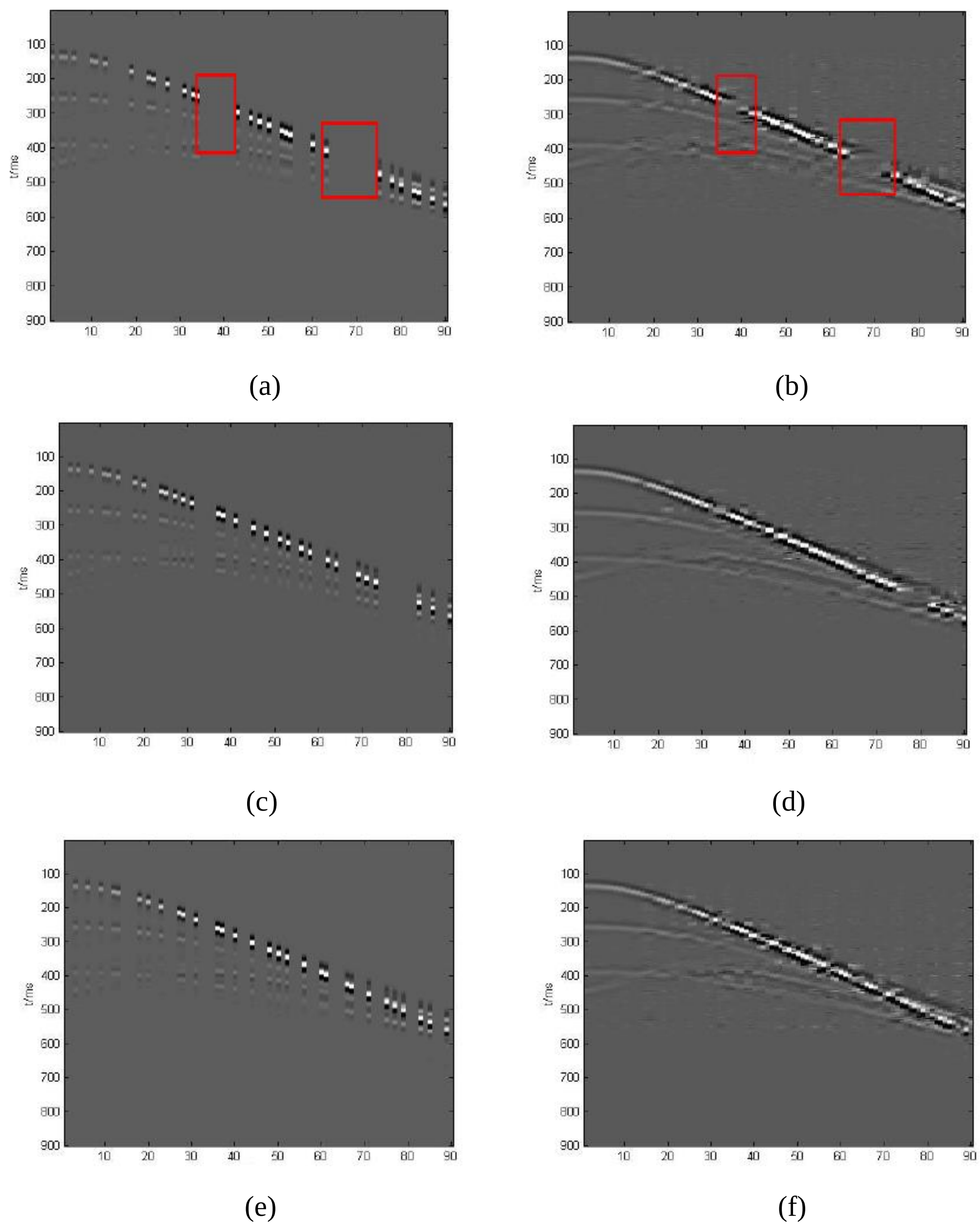

Figure 6: The comparison between the simulation results of three sampling methods under the sampling rate 25%. (a) Random undersampling. (b) Reconstruction result of random undersampling. (c) Jittered undersampling. (d) Reconstruction result of jittered undersampling. (e) LDPC matrix sampling. (f) Reconstruction result of LDPC matrix sampling

Table 2: SNR of three kinds of sampling simulation data under 25% of the sampling rate

Sampling method	Random sampling	Jittered sampling	LDPC sampling
Original signal	1. 536	1.587	1.632
Reconstructed SRN	3.021	4.236	4.563

We use the dictionary trained in the complete seismic record in Fig. 5(b) to sparsely represent the missing data and reconstruct it with FISAT. It can be seen from the Fig. 6 and Tab. 2 that the SNR obtained after reconstruction in the three sampling modes is not much lower, even if the low sampling rate is only 25% and the data SNR is about 1.5 db. The random sampling result is not much improved, and the sampling interval is easy to occur at low sampling rate. In the big case, the collection points are gathered in one place, which directly leads to the lack of large-scale data and which is difficult to reconstruct completely. The jitter method and the LDPC matrix improve this problem. The jitter sampling method has a significant improvement over the random sampling. The result of the LDPC method reconstruction and the jitter are almost slightly improved.

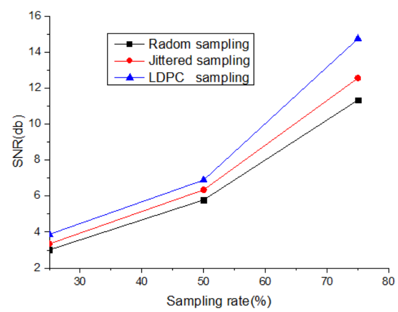

Figure 7: The SNR of reconstructed data with 25%, 50%, 75% sampling

Fig. 7 is a line graph of 25%, 50%, 75% sampling, and reconstructed data SNR for the whole data. In order to ensure the accuracy of the results and eliminate random interference, we still perform 50 times of data. The experiment was then averaged. It can be seen from the Fig. 7 that the SNR of the three methods increases correspondingly with the increase of the sampling rate. Whether it is low sampling rate or high sampling rate, the SNR of the LDPC matrix sample proposed in this paper is the highest, and the reconstruction result is the best.

4 Conclusion

This paper first analyzes the requirements of the applicable sampling matrix in seismic exploration, and shows the limitations of matrix usage in this field. Then, the existing acquisition methods are classified and described, because LDPC has as a compressed sensing sampling matrix. Due to its nature and in line with the requirements of seismic exploration, it is introduced into the three-dimensional exploration environment. We routinely propose a one-dimensional sampling method. The two-dimensional sampling is more in line with the actual exploration and has higher efficiency, eliminating the need for multiple measurements. The offline design steps have an advantage in the overall reconstruction of the data. In order to verify the effectiveness of our proposed method, we reconstruct the 3D simulation single-shot data in different acquisition modes, and then extract the same records from the 3D data for specific analysis, and sequentially increase the sampling rate to prove the validity of the results. Multiple experiments were performed in each case to avoid random errors. Then we use the actual data to perform the same operation in different ways. It can be seen from the experimental results that the proposed method has a relatively good effect. Generally, the method has certain practical application value.

Funding Statement: This study was supported by the Scientific Research Project of Hubei Provincial Department of Education (No. B2018029).

Conflicts of Interest: The authors declare that they have no conflicts of interest to report regarding the present study.

References

Anandakumar, H.; Umamaheswari, K. (2018): An efficient optimized handover in cognitive radio networks using cooperative spectrum sensing. *Intelligent Automation and Soft Computing*, vol. 24, no. 4, pp. 843-850.

Candes, E. J. (2008): The restricted isometry property and its implications for compressed sensing. *Comptes Rendus Mathematique*, vol. 346, no. 9-10, pp. 589-592.

Candes, E. J.; Romberg, J. K.; Tao, T. (2006): Stable signal recovery from incomplete and inaccurate measurements. *Communications on Pure and Applied Mathematics*, vol. 59, no. 8, pp. 1207-1223.

Candes, E. J.; Wakin, M. B. (2008): An introduction to compressive sampling: a sensing/ sampling paradigm that goes against the common knowledge in data acquisition. *IEEE Signal Processing Magazine*, vol. 25, no. 2, pp. 21-30.

Cheng, S. C.; Chen, G.; Wang, H. (2015): The preliminary study on high efficient acquisition of geophysical data with sparsity constraints. *Geophysical Prospecting for Petroleum*, vol. 54, no. 1, pp. 24-35.

Donoh, D. L. (2006): Compressed sensing. *IEEE Transactions on Information Theory*, vol. 52, no. 4, pp. 1289-1306.

Eldar, L.; Ozols, M.; Thompson, K. (2020): The need for structure in quantum LDPC codes. *IEEE Transactions on Information Theory*, vol. 66, no. 3, pp. 1460-1473.

Hennenfent, G.; Herrmann, F. J. (2008): Simply denoise: wavefield reconstruction via jittered under sampling. *Geophysics*, vol. 73, no. 3, pp. V19-V28.

Liu, C. J.; Wu, X. L.; Mo, B.; Zhang, Y. (2018): Multi-phase oil tank recognition for high resolution remote sensing images. *Intelligent Automation and Soft Computing*, vol. 24, no. 3, pp. 663-670.

Ma, J. W. (2011): Sparsity-promoting seismic exploration. *Proceedings of the 27th Annual Meeting of China Geophysical Society (in Chinese)*. Changsha.

Marks, R. J. (1991): *Introduction to Shannon Sampling and Interpolation Theory*. Springer, Verlag, USA.

Milton, A.; Trickett, S.; Burroughs, L. (2011): Reducing acquisition costs with random sampling and multidimensional interpolation. *81st International Annual Meeting, SEG, Expanded Abstracts*, pp. 52-56.

Moldoveanu, N. (2010). Random sampling: a new strategy for marine acquisition. *Proceedings of the SEG Annual Meeting, Society of Exploration Geophysicists*, pp. 51-55

Mosher, C. C.; Kaplan, S. T.; Janiszewski, F. D. (2012): Non-uniform optimal sampling for seismic survey design. *Expanded Abstracts of EAGE Annual Conference*, pp. 77-84.

Su, J.; Chen, Y; Sheng, Z.; Liu, A. (2020): From M-ary query to bit query: a new strategy for efficient large-scale RFID identification. *IEEE Transactions on Communications*, pp. 1-13.

Su, J.; Sheng, Z.; Leung, V. C. M.; Chen, Y. (2019): Energy efficient tag identification algorithms for RFID: survey, motivation and new design. *IEEE Wireless Communications*, vol. 26, no. 3, pp. 118-124.

Su, J.; Sheng, Z.; Liu, A.; Fu, Z.; Chen, Y. (2020): A time and energy saving based frame adjustment strategy (TES-FAS) tag identification algorithm for UHF RFID systems. *IEEE Transactions on Wireless Communications*, pp. 1-13. (in press)

Su, J.; Sheng, Z.; Liu, A.; Han, Y.; Chen, Y. (2019): A group-based binary splitting algorithm for UHF RFID anti-collision systems. *IEEE Transactions on Communications*, pp. 1-14, (in press).

Su, J.; Sheng, Z.; Xie, L.; Li, G.; Liu, A. (2019): Fast splitting based tag identification algorithm for anti-collision in UHF RFID system. *IEEE Transactions on Communications*, vol. 67, no. 3, pp. 2527-2538.

Tang, G. (2010): *Seismic Data Reconstruction and Denoising Based on Compressive Sensing and Sparse Representation (Ph.D. Thesis)*. Tsinghua University, China.

Lin, T.; Herrmann, F. J. (2009): Unified compressive sensing framework for simultaneous acquisition with primary estimation. *International Exposition and 79th International Annual Meeting, SEG, Expanded Abstracts*, pp. 3113-3117.

Wang, B.; Geng, J. (2020): Efficient deblending in the PFK domain based on Compressive sensing. *IEEE Transactions on Geoscience and Remote Sensing*, vol. 58, no. 2, pp. 995-1003.

Yang, M.; Zhang, W.; Zhong, J. (2013): Quasi-cyclic multiary LDPC code construction. *Journal of Electronics & Information Technology*, vol. 2, pp. 297-302.

Zhang, K. H.; Li, K. Q. (2018): The optimization reachability query of large scale multi-attribute constraints directed graph. *Computer Systems Science and Engineering*, vol. 33, no. 2, pp. 71-85.